Integrin-linked kinase is required for epidermal and hair follicle morphogenesis

Katrin Lorenz,[1] Carsten Grashoff,[1] Robert Torka,[1] Takao Sakai,[1] Lutz Langbein,[2] Wilhelm Bloch,[3] Monique Aumailley,[4] and Reinhard Fässler[1]

[1]Department of Molecular Medicine, Max Planck Institute of Biochemistry, D-82152 Martinsried, Germany
[2]Division of Cell Biology, German Cancer Research Center, D-69120 Heidelberg, Germany
[3]Department of Molecular and Cellular Sport Medicine, German Sport University Cologne, 50933 Cologne, Germany
[4]Department of Biochemistry, University of Cologne, 50923 Cologne, Germany

Integrin-linked kinase (ILK) links integrins to the actin cytoskeleton and is believed to phosphorylate several target proteins. We report that a keratinocyte-restricted deletion of the ILK gene leads to epidermal defects and hair loss. ILK-deficient epidermal keratinocytes exhibited a pronounced integrin-mediated adhesion defect leading to epidermal detachment and blister formation, disruption of the epidermal–dermal basement membrane, and the translocation of proliferating, integrin-expressing keratinocytes to suprabasal epidermal cell layers.

The mutant hair follicles were capable of producing hair shaft and inner root sheath cells and contained stem cells and generated proliferating progenitor cells, which were impaired in their downward migration and hence accumulated in the outer root sheath and failed to replenish the hair matrix. In vitro studies with primary ILK-deficient keratinocytes attributed the migration defect to a reduced migration velocity and an impaired stabilization of the leading-edge lamellipodia, which compromised directional and persistent migration. We conclude that ILK plays important roles for epidermis and hair follicle morphogenesis by modulating integrin-mediated adhesion, actin reorganization, and plasma membrane dynamics in keratinocytes.

Introduction

The skin is composed of an epithelial (epidermis and hair follicle [HF]) and a mesenchymal compartment (dermis, subcutis, and dermal papilla [DP]) joined and maintained together by a basement membrane (BM). The interfollicular epidermis contains multiple layers of keratinocytes at different stages of differentiation, from a basal layer of undifferentiated, proliferating keratinocytes attached to the BM, to terminally differentiated, cornified cells (Fuchs and Raghavan, 2002). The HF is an epidermal appendage, which arises as an epithelial cone from the fetal epidermis after a series of epithelial–mesenchymal cues. The mature HF epithelium consists of a central hair shaft (HS), surrounded by an inner and an outer root sheath (IRS and ORS, respectively). HS and IRS differentiation from the hair matrix (HM) is induced by mesenchymal cues from the connective tissue sheath and the DP. The mature HF has the ability to involute and regenerate, with cyclically alternating periods of rapid growth (anagen), apoptosis-driven regression (catagen), and relative quiescence (telogen). During each growth period, the progeny (transient amplifying [TA] cells) of epithelial stem cells located in the bulge region of the ORS extends into the mesenchymal compartment and generates a new HM. Here, epithelial cells change migration direction and terminally differentiate into IRS or HS (Paus and Cotsarelis, 1999).

Basal keratinocytes express several integrins, including $\alpha2\beta1$, $\alpha3\beta1$, $\alpha9\beta1$, $\alpha v\beta5$, and $\alpha6\beta4$ integrins (Watt, 2002). The $\alpha6\beta4$ integrin is the core component of hemidesmosomes anchoring keratin filaments to the BM, whereas $\alpha3\beta1$ and $\alpha9\beta1$ integrins link the actin cytoskeleton to the BM. The $\alpha2\beta1$ is found around the entire basal keratinocytes, where it is thought to mediate cell–cell interactions. ORS cells express $\alpha2\beta1$, $\alpha3\beta1$, and $\alpha6\beta4$ integrins at different levels according to the region of the HF (Commo and Bernard, 1997). In vitro studies with keratinocytes and genetic manipulations in mice revealed that $\beta1$ integrins regulate adhesion and differentiation of epidermal cells and play an essential role for hair germ invagination, ORS cell migration, and sustained HM proliferation during HF

K. Lorenz, C. Grashoff, and R. Torka contributed equally to this paper.

Correspondence to Reinhard Fässler: faessler@biochem.mpg.de

Abbreviations used in this paper: BM, basement membrane; DEJ, dermal–epidermal junction; DP, dermal papilla; FA, focal adhesion; FC, focal complex; GSK, glycogen synthase kinase; HF, hair follicle; HM, hair matrix; HS, hair shaft; ILK, integrin-linked kinase; IRS, inner root sheath; ORS, outer root sheath; P, postnatal day; PKB, protein kinase B; TA, transient amplifying.

The online version of this article contains supplemental material.

The Journal of Cell Biology, Vol. 177, No. 3, May 7, 2007 501–513
http://www.jcb.org/cgi/doi/10.1083/jcb.200608125

morphogenesis (Brakebusch et al., 2000; Raghavan et al., 2000; Watt, 2002; Grose et al., 2002). An important and still largely unanswered question is how integrins mediate these functions in skin and HFs. Because integrin cytoplasmic domains lack actin binding sites and enzymatic activity, signaling is implemented through accessory molecules such as talin, α-actinin, and integrin-linked kinase (ILK; Brakebusch and Fässler, 2003). ILK is composed of N-terminal ankyrin repeats, a pleckstrin homology–like domain and a putative, C-terminal kinase domain (Hannigan et al., 1996; Grashoff et al., 2004, Legate et al., 2006). ILK was given its name based on the enzymatic activity of its kinase domain (Delcommenne et al., 1998; Novak et al., 1998; Persad et al., 2000), which was shown to phosphorylate several target proteins, including protein kinase B (PKB)/Akt and glycogen synthase kinase (GSK) 3β. The significance of the ILK activity, however, is controversial as in vitro and in vivo results in flies, worms, and mice point toward an adaptor rather than an enzymatic function of ILK (Lynch et al., 1999; Zervas et al., 2001; Mackinnon et al., 2002; Hill et al., 2002; Grashoff et al., 2003; Sakai et al., 2003). A recent report proposed that the ILK activity is biologically relevant for transformed epithelial cells but not normal cells (Troussard et al., 2006). Whether the controversy may indeed be ascribed to the different biological systems used in the past to investigate ILK function awaits further studies. Another important function of ILK is its ability to link integrins to the actin cytoskeleton and to modulate actin reorganization (Zervas et al., 2001; Mackinnon et al., 2002; Grashoff et al., 2003; Sakai et al., 2003). Almost all proteins that bind ILK bind and/or regulate actin dynamics. They include PINCH1 and PINCH2, which bind actin modulators and connect ILK to growth factor receptors, the parvin family of F-actin binding proteins, and paxillin, which recruits actin binding and regulatory proteins, including vinculin, talin, α-actinin, and FAK (for reviews see Grashoff et al., 2004; Legate et al., 2006). HF development and cycling is crucially dependent on the inactivation of GSK-3β in HM cells (Fuchs et al., 2001; Huelsken et al., 2001). Active, nonphosphorylated GSK-3β can phosphorylate β-catenin bound to a protein complex, collectively called the β-catenin degradation complex. Phosphorylation of GSK-3β inactivates the kinase and leads to stabilization and translocation of β-catenin to the nucleus, where it associates with the Lef1/Tcf family of DNA binding proteins to activate the transcription of target genes, such as cyclin D1, c-myc, homeobox containing transcription factors, Lef1, and hair-specific keratins (Zhou et al., 1995; for review see Logan and Nusse, 2004). ILK can modulate the stability of β-catenin either through phosphorylating GSK-3β (Delcommenne et al., 1998; Novak et al., 1998) or through inhibiting the β-catenin degradation complex (Oloumi et al., 2006) and could therefore play a central role for HF morphogenesis.

To test the function of ILK during epidermis and HF development, we deleted the ILK gene in keratinocytes. We found that loss of ILK compromises epidermal keratinocyte adhesion and disrupts HF formation, leading to progressive hair loss. The HF defect was not due to an abnormal β-catenin stability, HM differentiation, or stem cell maintenance. Instead, the accumulation of proliferating ORS cells points to an impaired HF downward growth in vivo.

Results

Deletion of ILK in keratinocytes leads to progressive hair loss

To delete the ILK gene in keratinocytes, floxed ILK mice were intercrossed with animals carrying the keratin 5 (K5)–Cre transgene (ILK-K5 mice). Littermates carrying heterozygous floxed

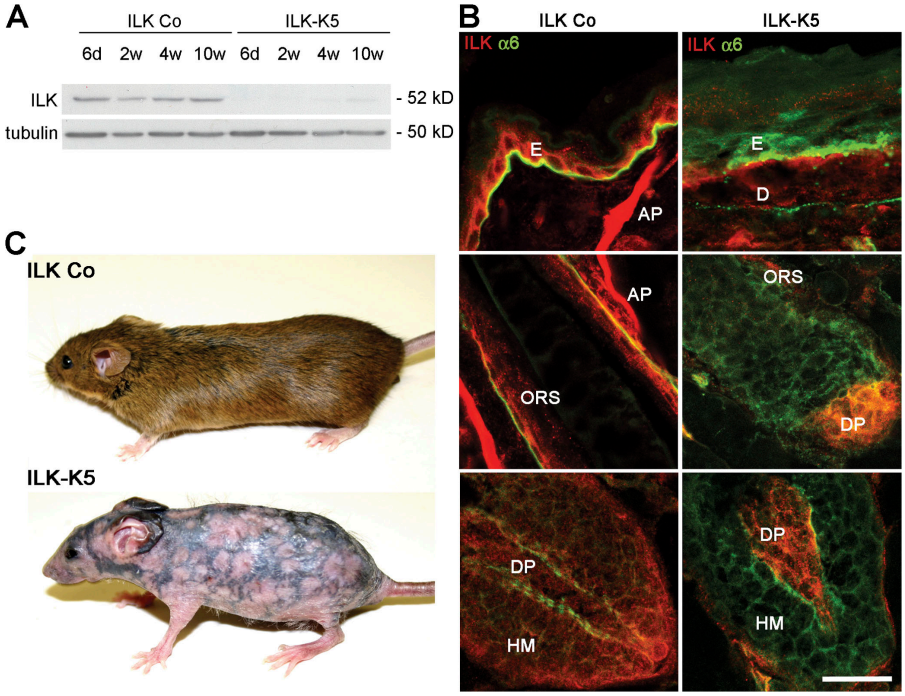

Figure 1. **Keratinocyte-restricted deletion of ILK causes progressive hair loss.** (A) ILK protein level in epidermal lysates of ILK Co and ILK-K5 mice. (B) Back skin of 2-wk-old ILK Co and ILK-K5 animals stained for ILK and α6 integrin. ILK is expressed in basal keratinocytes of the epidermis (E), ORS, HM, DP, arrector pili muscle (AP), and dermis (D). ILK-K5 skin retains ILK expression in DP and dermis but lacks ILK expression in epidermis, HM, and ORS. Bar, 25 μm. (C) Control and ILK-K5 animals at 8 wk of age.

ILK gene and the K5-Cre transgene served as controls (ILK Co). K5-mediated Cre expression deleted the ILK gene in back skin at around embryonic day 15, decreased ILK levels in newborn skin, and led to the loss of the ILK protein thereafter (Fig. S1 A, available at http://www.jcb.org/cgi/content/full/jcb.200608125/DC1). Western blot analysis in back skin epidermis of 6-d-, 2-wk-, 4-wk-, and 10-wk-old mice confirmed the sustained absence of ILK (Fig. 1 A). Immunostained sections of 2-wk-old control mice revealed ILK in basal epidermal keratinocytes, ORS, HM, DP, and the arrector pili muscle (Fig. 1 B). ILK was absent from epidermis and HF epithelium of ILK-K5 skin but still present in DP (Fig. 1 B).

ILK-K5 animals were indistinguishable from control littermates at birth. At 1–2 wk, when control animals developed their hair coat, ILK-K5 animals had scattered hair with partial alopecia. This appearance endured until around 4 wk of age and was followed by progressive hair loss, leading to persistent alopecia by 6–8 wk (Fig. 1 C). A reticular pigmentation pattern developed on the back skin of 8-wk-old ILK-K5 mice (Fig. 1 C), whereas hair coat and hair cycle–dependent skin color changes occurred normally in control mice.

Loss of ILK causes severe epidermal and HF abnormalities

The epidermis of ILK-K5 mice was morphologically normal at birth and postnatal day (P) 2 but became progressively hyperplastic (at P7–9, four to five cell layers, and at P28, six to seven cell layers; Fig. 2, A and B). Although basal keratinocytes were polarized and tightly attached to the BM in control skin, they appeared flattened in the mutant epidermis and were often detached along the dermal–epidermal junction (DEJ; Fig. 2, A and B, asterisks). The detachment became more severe with age (at P7, 5–10% of total epidermal length; at P14, 30–50%; and at P70, up to 70%) but did not result macroscopically in visible skin blisters.

The most striking phenotype was a severe impairment of HF development in ILK-K5 mice characterized by a progressive growth retardation, which was first visible at around P2 (Fig. 2, A and D). By P14, control mice had completed HF morphogenesis, with all hair bulbs residing deep in the subcutis. In contrast, ILK-K5 HFs diverged into two subpopulations. (1) Approximately 33% of the mutant HFs reached the final stages of HF morphogenesis but were shortened and profoundly distorted. They displayed substantial hyperplasia of the ORS with up to six cell layers and condensed DPs (Fig. 2, A, C, and D, ▲). (2) Approximately 66% of the mutant HFs were arrested in their development. They failed to reach down deeper than the reticular dermis and showed defective morphogenesis with distorted or absent HS formation and misshapen HM and DP (Fig. 2, A, C, and D, ■). A plausible explanation for the varying HF populations is the combination of an asynchronous HF morphogenesis (Paus et al., 1999) and the perinatal loss of ILK protein

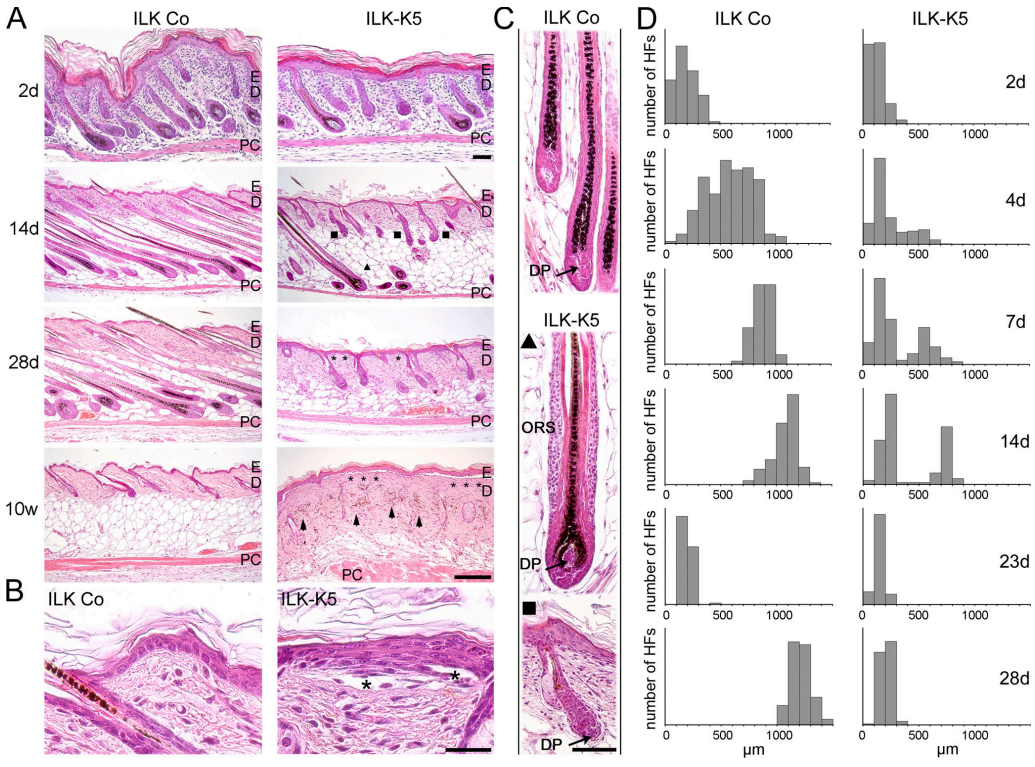

Figure 2. **Keratinocyte-restricted deletion of ILK leads to epidermal hyperplasia and epidermolysis and perturbs HF development and growth.** (A) Hematoxylin-eosin staining of sections derived from back skin of control and ILK-K5 mice. ILK-K5 mice display stunted HF morphogenesis leading to two HF types (▲, fully developed; ■, shortened and prematurely arrested), progressive epidermal detachment (asterisks), and dermal pigment deposition (arrowheads). Bar, 100 µm. (B) Epidermis from 2-wk-old ILK-K5 mice is hyperplastic and detached from the underlying dermis (asterisks). ILK-K5 keratinocytes show a flattened morphology. Bar, 25 µm. (C) High magnification of hematoxylin-eosin–stained HFs from 9-d-old back skin. ILK-K5 HFs have multilayered ORS (▲) or show premature growth arrest with loosely attached, malformed DP (arrow; ■). Bar, 50 µm. (D) ILK-K5 HF growth is perturbed during morphogenesis and cycling. HF lengths of a minimum of 100 HFs per time point are presented as histograms. PC, panniculus carnosum; E, epidermis; D, dermis.

expression: fully developed HFs (Fig. 2, ▲) lost ILK late in morphogenesis, whereas arrested HFs (■) lost ILK early in morphogenesis. At P28, none of the ILK-K5 HFs was able to initiate anagen characterized by HF downgrowth into the subcutis (Fig. 2, A and D). By 10 wk of age, the ILK-K5 HFs were resorbed (Fig. 2 A) and melanin condensates within the dermis gave rise to a reticular skin pigmentation (Fig. 1 C).

Loss of ILK compromises keratinocyte adhesion and BM maintenance

Cell detachment in ILK-K5 skin points to a compromised integrin function that could be caused by altered expression, activity, localization, or weaker linkage to the actin cytoskeleton. Integrin function was tested with adhesion assays using fibronectin (FN), collagen I (Col I), collagen IV (Col IV), and laminin 332 (LM332) as substrates. Although interaction with poly-L-lysine was similar between ILK-K5 and control keratinocytes, adhesion to the ECM substrates was significantly diminished in ILK-K5 keratinocytes (Fig. 3 A).

Integrin expression determined by FACS revealed strong β1 integrin expression and a comparable Mn^{2+}-triggered activation of β1 integrins on freshly isolated control and ILK-K5 keratinocytes. However, a subpopulation of ILK-K5 cells expressed lower levels of β1 integrin (Fig. S1 B). The expression levels of the α6, β4, and αv integrin subunits were not changed on ILK-K5 keratinocytes, whereas the α3 and α2 integrin chains were slightly up-regulated (Fig. S1 B). In situ immunostaining revealed differences in integrin localization at the cellular level. In control skin, β1 integrin was expressed around the entire surface of basal keratinocytes (Fig. 3 B) and β4 and α6 integrins along the DEJ (Fig. 3 B and Fig. 4). In ILK-K5 skin, the β1 integrin subunit was present on basal keratinocytes but also on many suprabasal cells (Fig. 3 B), which maintained K14 expression (Fig. 3 B, middle). The localization of α6 and β4 integrins on ILK-K5 basal keratinocytes was comparable to control skin, with the exception of a few areas lacking detectable α6 and β4 integrin and some suprabasal cells showing a strong staining for α6 and β4 integrin (Fig. 3 B). The latter cell population likely expressed similar levels of α6β4 integrins as basal keratinocytes, as FACS analysis of freshly isolated keratinocytes did not distinguish two populations of α6β4-expressing keratinocytes (Fig. S1 B).

The decreased keratinocyte adhesion was associated with severe BM defects. Although control skin showed a linear staining of LM332 along the DEJ and around HFs, ILK-K5 skin displayed irregular deposits of LM332 at the DEJ with areas of massive LM332 (Fig. 3 B, asterisks) diffusion into the dermis and dotlike deposits adjacent to integrin-positive suprabasal keratinocytes (Fig. 3 B, right, arrowhead). EM of a control skin revealed a regular BM structure at the DEJ, whereas mutant skin showed an abnormal BM with discontinuities in the lamina densa between hemidesmosomes (Fig. 3 C). The number of hemidesmosomes was normal except in areas with detached epidermis, where the number was reduced. Collectively, these data demonstrate that loss of ILK weakens integrin-mediated adhesion of basal keratinocytes to the BM and abrogates BM integrity.

ILK regulates proliferation and differentiation of epidermal keratinocytes

ILK-deficient epidermis was hyperplastic (Fig. 2 A). Ki67 immunostaining revealed that P4 epidermis from control as well as

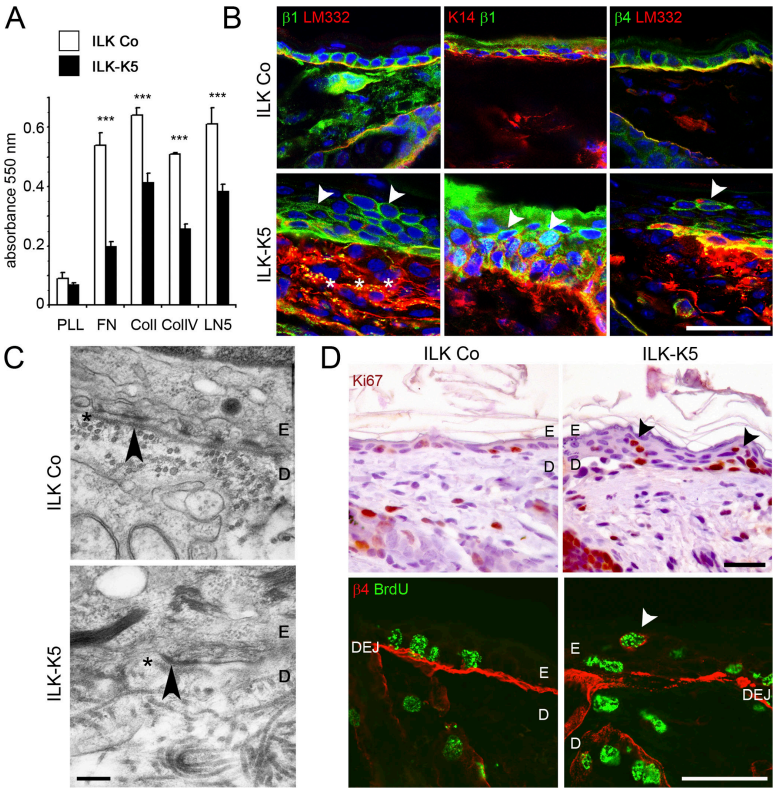

Figure 3. **ILK ablation impairs keratinocyte adhesion, integrin expression, and BM integrity and alters proliferation in vivo.** (A) Cell adhesion of ILK-K5 keratinocytes from 4-d-old mice on FN, Col I, Col IV, and LM332 is significantly reduced compared with control keratinocytes. Adhesion to poly-L-lysine (PLL) is not different (mean + SD of three independent experiments; ***, $P < 0.001$). (B) Integrin expression in epidermis from 2-wk-old mice. In control skin, β1 and β4 integrins are expressed in basal keratinocytes, whereas in ILK-K5 skin both integrins are also found on suprabasal keratinocytes (arrowheads). In ILK-K5 mice, β4 integrin shows discontinuous staining on basal keratinocytes, LM332 diffuses into the upper dermis (asterisks), and β1 integrin–expressing suprabasal cells retain K14 expression. Bars, 25 μm. (C) Electron micrographs of back skin sections of 2-wk-old control and ILK-K5 mice. Control skin exhibits a continuous lamina densa (asterisks) and hemidesmosomes (arrowhead), whereas ILK-K5 skin shows a discontinuous lamina densa, which is preserved at hemidesmosomes (arrowhead) but largely absent in between. Bar, 0.25 μm. (D) Ki67 staining revealed the presence of proliferating cells in ILK-K5 suprabasal layers. Suprabasal BrdU+ cells express β4 integrin. Bars, 25 μm.

ILK-K5 skin contained comparable numbers of proliferating cells almost exclusively in the basal layer. At P7, however, ILK-K5 skin contained normal numbers of proliferating cells in the basal layers and, in addition, a significant number of proliferating cells in the suprabasal layers (Fig. S2, A and B, available at http://www.jcb.org/cgi/content/full/jcb.200608125/DC1). The ectopic keratinocyte proliferation was also observed in Ki67-immunostained skin (Fig. 3 D). It occurred in areas with aberrant and normal BM and was associated with β1 and β4 integrin expression (Fig. 3 D).

To test whether loss of ILK expression also affected proliferation of primary keratinocytes in vitro, we performed BrdU incorporation assays. In three independent experiments, we found an increased incorporation of BrdU in ILK-K5 keratinocytes when compared with control cells (Fig. S2 C). Surprisingly, however, the phosphorylation of known ILK targets involved in cell cycle control, such as Ser9 of GSK-3β and Ser473 of PKB/Akt, and the expression of D-type cyclins were not changed in ILK-K5 epidermal lysates (Fig. S2 D).

The defective keratinocyte adhesion could trigger a chronic wound healing response with infiltrating inflammatory cells, which in turn may induce the ectopic proliferation of suprabasal keratinocytes in vivo. To test this, we searched skin sections from control and ILK-K5 mice for the presence of granulocytes and macrophages. As expected, granulocyte and macrophage infiltrates were absent from P7 as well as P14 control skin (Fig. S3, A and B, available at http://www.jcb.org/cgi/content/full/jcb.200608125/DC1). ILK-K5 skin also lacked granulocyte and macrophage infiltration at P7 (Fig. S3, A and B), when abundant proliferation of suprabasal keratinocyte was already evident (Fig. S2 B). At P14, however, macrophages accumulated around ILK-K5 HFs and granulocytes beneath the epidermis (Fig. S3, A and B).

The presence of proliferating, integrin-positive keratinocytes in suprabasal layers points to an aberrant differentiation and/or mislocalization of undifferentiated ILK-K5 keratinocyte. To investigate differentiation, we analyzed the expression of epidermal keratins. K14 was expressed in basal cells and weakly extended into the first suprabasal layer of control epidermis (Fig. 4 A). In ILK-K5 skin, K14 was expressed suprabasally in up to five cell layers (Fig. 4 A). Normal suprabasal cells switched off K14 and K5 expression and instead expressed K10 (Fig. 4 A). In ILK-K5 epidermis, K10 was absent from basal cells but strongly expressed in the four to five suprabasal cell layers. In addition, there were often patches of cells lacking K10 but expressing integrins (Fig. 4 A, asterisks) and high levels of K14 (Fig. 4 A and Fig. 3 B). Furthermore, although loricrin was confined to the stratum granulosum and appeared as a thin linear signal in control epidermis, in ILK-K5 epidermis, loricrin was found in two to three cell layers, which contained large and round keratinocytes with prominent nuclei (Fig. 4 A). These data suggest that loss of ILK sustains proliferation and expression of basal layer markers in suprabasal cell layers and delays keratinocyte differentiation.

ILK maintains polarity of epidermal keratinocytes

ILK-deficient keratinocytes have a flattened shape (Fig. 2 B), suggesting that their polarity was impaired. To investigate keratinocyte polarity in vivo, we compared F-actin and the distribution of cell–cell adhesion molecules between control and ILK-K5 epidermis. In control epidermis, F-actin distributed to the apical and lateral plasma membranes of basal keratinocytes, whereas in ILK-K5 epidermis, the F-actin was also present at the basal plasma membrane zone facing the BM, where it frequently colocalized with nidogen (Fig. 4 B). Similar F-actin defects were also seen in mutant HFs (Fig. 4 C).

In normal skin, E-cadherin and its junctional adaptor protein β-catenin were found at the lateral and apical plasma membrane of basal keratinocytes (Fig. 4 B and not depicted).

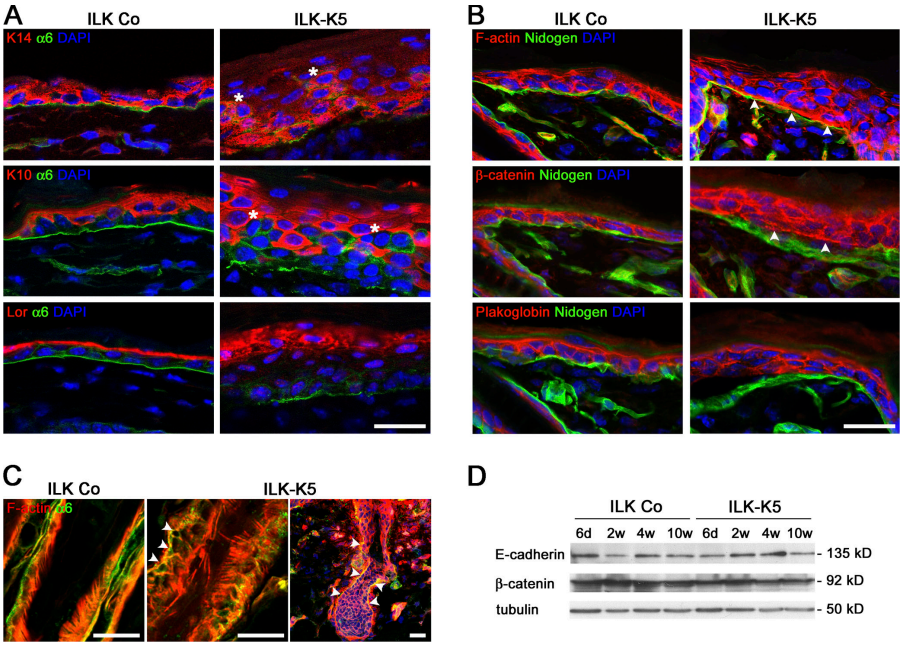

Figure 4. **Loss of ILK retards differentiation and disturbs polarity of epidermal keratinocytes.** (A) Double immunostaining for K14, K10, or loricrin (Lor) and α6 integrin on back skin of 2-wk-old control and ILK-K5 animals. ILK-K5 epidermis shows several cell layers expressing K14 and loricrin, respectively. Integrin α6 expression is discontinuous in ILK-K5 skin and present on suprabasal cells (asterisks). Bar 25 μm. (B) Immunostaining for F-actin, β-catenin, and plakoglobin in 2-wk-old mouse skin. In control epidermis, F-actin and β-catenin are absent from the basal side of basal keratinocytes. In ILK-K5 epidermis, F-actin and β-catenin are found basally adjacent to nidogen (arrowheads). Plakoglobin localizes to the lateral–apical sides of basal keratinocytes of both control and ILK-K5 mice. Bar, 25 μm. (C) F-actin overlaps with α6 integrin in the mutant HF (arrowheads). Bars, 50 μm. (D) Western blot analysis reveals similar expression levels of E-cadherin and β-catenin in control and ILK-K5 epidermal lysates.

In ILK-K5 skin, the E-cadherin and β-catenin staining was normally distributed in areas where the epidermis was attached to the dermis. In areas where the epidermis was detached from the BM, both E-cadherin and β-catenin were redistributed to the basal side of basal keratinocytes (Fig. 4 B and not depicted). In epidermal lysates, E-cadherin and β-catenin protein levels were indistinguishable between control and ILK-K5 samples (Fig. 4 D). The expression and localization of desmosomal components such as plakoglobin and desmoplakin (Fig. 4 B and not depicted), as well as the ultrastructure of desmosomes (Fig. S3 C), were unaffected in all areas of the ILK-K5 epidermis. We conclude that ILK controls cell polarity by maintaining the integrity of the actin cytoskeleton and BM and not by regulating E-cadherin expression or the formation of cell–cell junctions.

Loss of ILK permits normal β-catenin–Lef1 signaling and HF differentiation

A possible role of ILK for hair epithelium differentiation stems from the observation that ILK controls β-catenin–Lef1–mediated gene transcription either by phosphorylating and inactivating GSK-3β (Delcommenne et al., 1998) or by stabilizing β-catenin (Oloumi et al., 2006). To test whether GSK-3β and the downstream β-catenin–Lef1 complex were affected by the loss of ILK, we performed a series of different experiments. Immunoblotting of lysates from freshly isolated keratinocytes revealed that the total levels of GSK-3β and the extent of phosphorylation of Ser9 did not differ between control and ILK-K5 samples (Fig. S2 D). Immunostaining revealed that Lef1 and nuclear β-catenin were present in the precortical HM and HS cortex of control as well as fully developed ILK-K5 HFs (Fig. 5, A and B, ▲). Moreover, both proteins could clearly be detected in the Ki67-positive HM cells of prematurely growth-arrested ILK-K5 HFs (Fig. 5, A and B, ■). To determine the activity of the nuclear β-catenin–Lef1 transcription factor complex, ILK-K5 mice were intercrossed with reporter mice, in which β-galactosidase expression is controlled by nuclear β-catenin–Lef1 (Maretto et al., 2003). The expression of β-galactosidase was clearly visible in the HS of control and fully developed ILK-K5 HFs (Fig. 5 C, ▲) and in cells of growth-retarded ILK-K5 HFs (Fig. 5 C, ■). Normal activity of the β-catenin–Lef1 complex was further confirmed by determining the β-catenin–Lef1–dependent expression of IRS-specific keratins. The IRS keratin K6irs1 (Fig. 5 D) and K6irs2-4 (not depicted) were normally expressed in ILK-K5 HFs. Similarly, the expression of ORS keratins and several HS-specific markers (e.g., hHa1) was also normal in both populations of ILK-K5 HF (even though the localization of the K6irs1-positive cells in the shortened mutant HF was abnormal; Fig. 5 D). Altogether, these findings demonstrate that ILK regulates neither the phosphorylation of GSK-3β and the stability and activity of β-catenin in HFs nor the differentiation of HM into the IRS or HS.

ILK loss leads to accumulation and premature proliferation of ORS cells

Loss of β1 integrin expression leads to reduced proliferation of epidermal keratinocytes and HF matrix cells (Brakebusch et al., 2000; Raghavan et al., 2000). To assess whether altered proliferation of the ILK-K5 HM accounts for the abnormal hair

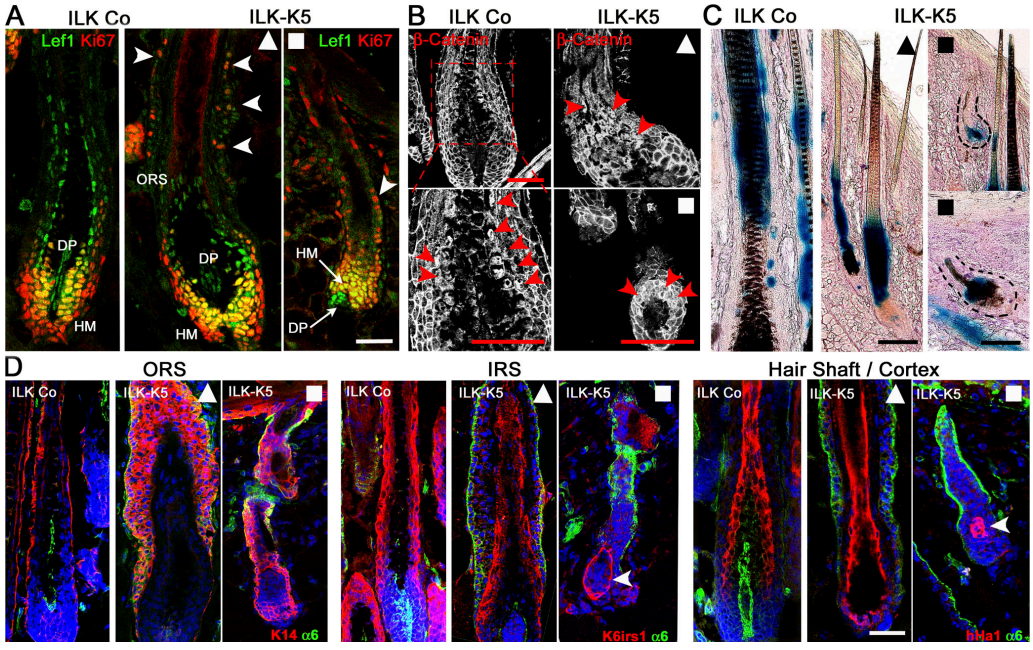

Figure 5. **ILK-K5 HFs show normal β-catenin stability and hair-specific differentiation.** (A) Control and mutant 2-wk skin sections stained for Ki67 and Lef1 show an increased number of Ki67+ cells in the ORS (arrowheads), yet retained Lef1 expression in the HM and DP of ILK-K5 HFs. (B) Control and mutant 2-wk skin sections stained for β-catenin revealed nuclear β-catenin (arrowheads) in precortical HM and proximal HS cortex in both control and long (▲) and short (■) ILK-K5 HFs. (C) BatGal reporter mice were intercrossed with ILK-K5 and control animals. LacZ activity is present in precortical HM and HS cortex of both control and ILK-K5 HFs. (D) Immunostaining of K14 for the ORS, of keratin K6irs1 for the IRS, and of keratin hHa1 for HS cortex and α6 integrin. ILK-K5 HFs revealed the presence of a multilayered K14+ ORS. K6irs1 and hHa1 were expressed but mislocalized in short ILK-K5 HFs (arrowheads). Bars, 50 μm.

development, we performed BrdU incorporation assays and determined Ki67 expression. At P7, both fully developed ILK-K5 HFs (Fig. 6 A, ▲) as well as growth-retarded HFs (Fig. 6 A, ■) showed an elevated number of proliferating cells in the ORS. To quantify the number of proliferating cells, we counted their numbers on fully developed ILK-K5 HFs (Fig. 6 A, ▲), thereby ensuring comparison of identical HF developmental stages. Counting of proliferating cells in P7 ILK-K5 HFs revealed that the increased number of proliferating ORS cells was associated with a slight but not significantly lower amount of proliferating cells in the HM (Fig. 6, B–D). At P14, however, the number of proliferating cells significantly diminished in the HM and further increased in the ORS (Fig. 6, B–D), suggesting that ILK-deficient, rapidly proliferating TA cells are capable of proliferating but accumulate in the ORS. Moreover, neither TUNEL assays nor immunostaining for activated caspase-3 revealed an elevation in apoptotic cell numbers, indicating that cell survival was unaffected in the ILK-K5 HFs (unpublished data).

The ORS cells originate from the CD34-positive stem cell population that is located in the hair bulge (Blanpain and Fuchs, 2006). To determine whether ILK loss led to the elimination of CD34-positive cells, we immunostained P24 skin sections. Both control and ILK-K5 HFs contained CD34-positive cells in their hair bulges (Fig. 6 E). The formation of secondary hair germs is driven by the proliferation of hair bulge-derived TA cells triggered by the inductive activity of the DP. At P24, normal HFs are at the onset of anagen, and Ki67+ TA cells appeared adjacent to the DP (Fig. 6 F, left). Ki67 staining of ILK-K5 skin revealed the presence of two types of HFs: ~65% contained proliferating cells, suggesting that ILK-K5 HFs were principally capable of entering early stages of anagen (Fig. 6 F, middle). The remaining ILK-K5 HFs lacked proliferating cells (Fig. 6 F, right), likely because they were detached from the DP (Fig. 6 E, right) or connected to a malformed DP (Fig. 2 C) and, hence, did not receive the inductive signals. Collectively, these data suggest that ILK-K5 HFs contain CD34-positive stem cells that give rise to TA cells, which require ILK to migrate down to the HM or to trigger the downward growth of hair germs.

ILK is required for directional migration of keratinocytes

In ILK-K5 HFs, rapidly proliferating TA cells accumulate in the ORS, suggesting that ILK regulates their migration along the LM332-containing BM lining the HF. To test this assumption, we isolated keratinocytes from control and ILK-K5 mice and compared their migration behavior using different assays.

We first performed transwell migration assays and observed that migration of primary ILK-K5 keratinocytes on LM332, as well as their invasion through laminin-rich matrigel, was significantly impaired (Fig. 7 A). Next, we scratched monolayers of primary keratinocytes and observed the closure of the scratch over 12 h using time-lapse video microscopy.

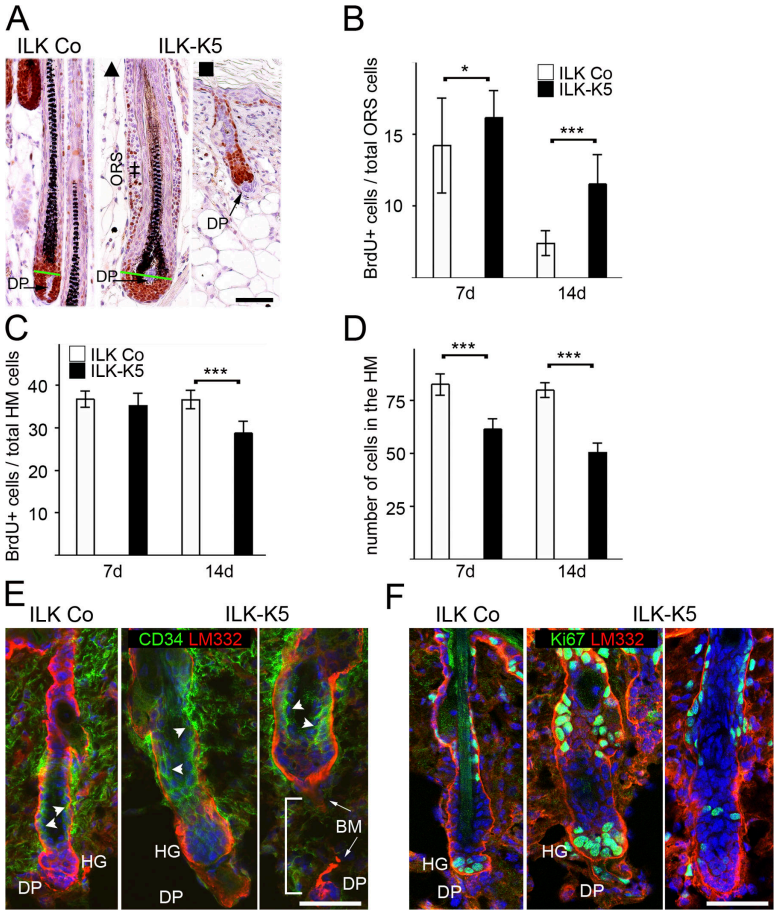

Figure 6. **ILK-deficient HFs accumulate proliferating cells in the ORS.** (A) Fully developed ILK-K5 HFs display a hyperplastic ORS (++). Both types of ILK-K5 HFs (▲, ■) show an elevated number of Ki67-positive ORS cells. Auber's line (green line; Auber, 1952) demarks the border between the proliferative and nonproliferative zones of the HM. Bar, 50 µm. (B) Quantification of BrdU+ cells in ILK Co and ILK-K5 HFs as a percentage of total cells in the ORS. The number of proliferating cells in the ORS is significantly increased in mutant HFs. (C) The percentage of proliferating cells in the HM is normal in 7-d HFs but significantly reduced in 14-d ILK-K5 HFs. (D) The overall number of cells is significantly reduced in the HM of 7- and 14-d ILK-K5 HFs. A minimum of 25 HFs were evaluated for B, C, and D at each time point (error bars indicate 95% confidence interval of mean values; *, $P < 0.05$; ***, $P < 0.001$). (E) Double immunostaining of CD34 and LM332 on skin sections of 24-d-old animals reveals the presence of a CD34+ bulge region (arrowheads) in ILK Co as well as ILK-K5 HFs. Note that ILK-K5 HFs display a severely abnormal morphology at this stage sometimes with detached DP (bracket). Bar, 25 µm. (F) Double immunostaining of Ki67 and LM332 on skin sections of 24-d-old animals. Proliferating hair germ is formed in HFs with DP and absent in ILK-K5 HFs without DP. HG, hair germ. Bar, 25 µm.

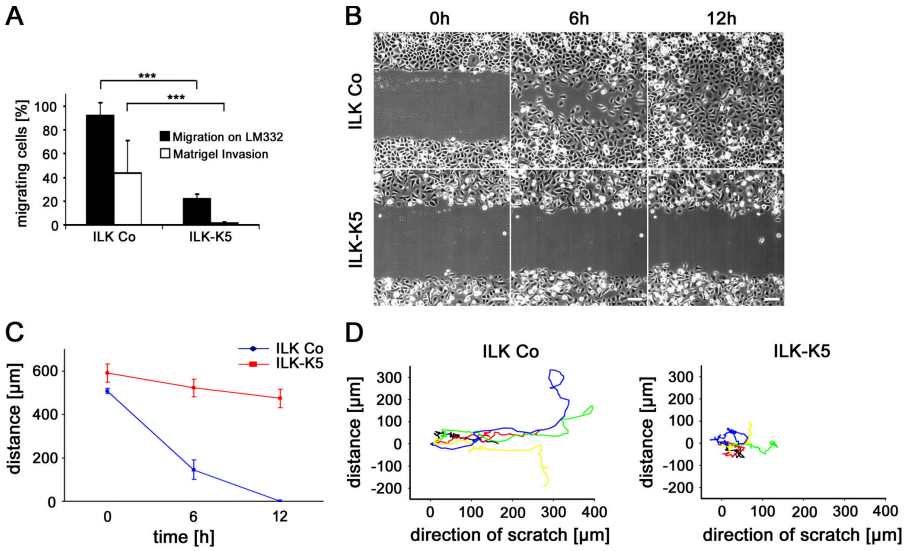

Figure 7. **Loss of ILK impairs migration.** (A) Freshly isolated keratinocytes were subjected to migration on LM332 and invasion through Matrigel. ILK-K5 keratinocytes show impaired migration and invasion (mean + SD of three independent experiments; ***, $P < 0.001$). (B) Time-lapse microscopy of a scratch assay. ILK-K5 keratinocyte exhibit delayed wound closure. Bar, 100 µm. (C) Quantification of the wound closure in the scratch assay. ILK-K5 wound closure is retarded (error bars indicate 95% confidence interval of mean values). (D) Reduced directionality of single ILK-K5 keratinocytes in the leading front of keratinocytes after scratch induction (five representative cells selected out of 40 analyzed for each genotype).

After scratching, control keratinocytes displayed directional migration and invaded the denuded area (Fig. 7, B and D) with a mean wound closure speed of 42.3 µm/h, leading to the closure of the scratch within 12 h (Fig. 7 C). In contrast, ILK-K5 keratinocytes often stopped and migrated back- and sideward (Fig. 7 D), with a reduced wound closure speed of 9.7 µm/h (Fig. 7, B and C). Furthermore, single-cell tracking at the migration front revealed a migration velocity of 0.7 ± 012 µm/min by ILK-K5 keratinocytes versus 0.9 ± 016 µm/min by control cells ($P < 0.01$).

To more closely evaluate the migration defect, we performed time-lapse microscopy of single keratinocytes. Control keratinocytes formed broad, usually single and stable leading edge lamella with a mean persistence of 985 ± 339 s that allowed single cells to directionally migrate (Fig. 8, A and B; and Video 1, available at http://www.jcb.org/cgi/content/full/jcb.200608125/DC1). In sharp contrast, ILK-K5 lamellae were instable and collapsed within 618 ± 332 s (Fig. 8 B). Furthermore, the mutant cells constantly extended new lamellae toward different directions simultaneously, which gave rise to frequent changes of the migration direction and consequently prohibited directional movement (Fig. 8 A and Video 2).

To precisely characterize lamellipodia behavior, we monitored and quantified the plasma membrane extension rates of migrating cells using kymography (Hinz et al., 1999) over a period of 20 min. The lamellipodia of ILK-K5 keratinocytes persisted for a significantly shorter time (Fig. 8 C) and protruded more frequently than those of control keratinocytes (Fig. 8 D). Collectively, these data indicate that ILK is important for the stability and dynamics of the lamellae/lamellipodia and hence for directional migration of keratinocytes.

Loss of ILK leads to reduced spreading, focal adhesion (FA) formation, and FAK activation

The reduced adhesion of ILK-K5 keratinocytes to the ECM (Fig. 2 B and Fig. 3 A) can diminish the fixation of plasma membrane protrusions to the ECM, impair cytoskeletal reorganizations, and compromise integrin-triggered signaling, which in turn can cause the abnormal formation of leading-edge lamellipodia and impaired directional migration.

To test whether ILK is critical for the formation of integrin adhesion sites and integrin signaling, we isolated control and ILK-K5 keratinocytes. Both cultured cell types had comparable integrin profiles, β1 integrin activity, and α6β4-containing migration track patterns at the rear of the cell (Fig. S4, A and B, available at http://www.jcb.org/cgi/content/full/jcb.200608125/DC1). The size of ILK-K5 cells was smaller, reaching a threefold smaller spreading area 40 h after plating on a mixture of Col I and FN (Fig. S4 C). Talin staining of adherent cells revealed that ILK-K5 keratinocytes formed fewer

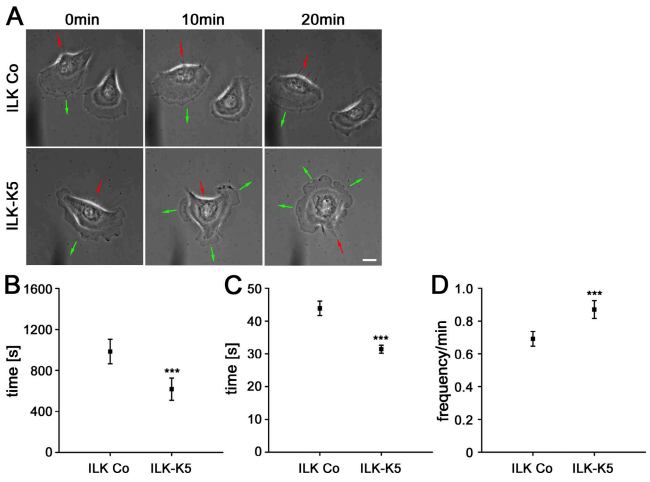

Figure 8. **ILK-K5 keratinocytes exhibit reduced lamellipodia stability.** (A) Time-lapse microscopy of single control and ILK-K5 keratinocytes. ILK-K5 keratinocytes formed instable lamellipodia, leading to a constant change of direction (green arrows indicate the protrusion and red arrows the retraction of the cell). Single frames chosen from Videos 1 and 2 (available at http://www.jcb.org/cgi/content/full/jcb.200608125/DC1). Bar, 10 µm. (B) Quantification of lamella stability. ILK-K5 keratinocytes exhibit significantly reduced lamella stability. (C and D) Quantification of lamellipodia persistence (C) and lamellipodia frequency (D). Compared with control keratinocytes, ILK-K5 lamellipodia protrusions are significantly less stable and occur more frequently. Error bars in indicate 95% confidence interval of mean values. ***, $P < 0.001$.

focal complexes (FCs) in the leading-edge lamellipodia (Fig. 9 A). Additional immunostaining for paxillin and FAK showed that only 30% of the cells contained mature FAs (Fig. 9, B and D) whose number per cell and size were significantly reduced (Fig. 9 C). The number of FAs in relation to the cell contact area, however, was not altered between ILK Co and ILK-K5 keratinocytes. In line with the severe spreading defect, ILK-K5 keratinocytes contained fewer stress fibers than control cells (Fig. 9, A, B, and D).

ILK can associate with several FA components, which in turn can modulate the activity of adaptor and signaling proteins, including FAK and Rac1 (Legate et al., 2006). Therefore, we tested whether their function is affected in ILK-K5 cells. Although total FAK levels were normal in ILK-K5 keratinocytes, the auto-activated form of FAK (pY397-FAK), as well as other tyrosine residues, such as Y861, were reduced (Fig. 9 E).

To test whether Rac-1 can be activated upon cell adhesion, we determined the levels of GTP-loaded Rac1 before and after cell seeding on LM322. Both ILK-K5 and control keratinocytes activated Rac1 to a similar extent (Fig. 9 F), indicating that the absence of ILK does not impair Rac1 activation in keratinocytes. Moreover, growth factor–induced activation of Rac1 became similarly increased in control and ILK-K5 keratinocytes (unpublished data).

Discussion

In the present paper, we report that a keratinocyte-restricted deletion of the ILK gene in mice leads to abnormal HF morphogenesis and epidermal defects with blisters, ectopic keratinocyte proliferation in suprabasal cell layers, and abnormal keratinocyte differentiation. Mutant HFs produced proliferating progenitor cells, which accumulated in the ORS and failed to replenish the HM. In vitro experiments revealed that ILK-deficient keratinocytes were unable to firmly stabilize lamellipodia, leading to impaired directional migration and providing a potential explanation for the accumulation of progenitor cells in the ORS.

Epidermal morphogenesis

The most prominent defects of the ILK-deficient epidermis were detachment from the dermal–epidermal BM and hyperthickening. The hyperthickened epidermis contained a normal number of proliferating keratinocytes in the basal layer and, surprisingly, also proliferating keratinocytes ectopically in the suprabasal layers. The cycling cells in the suprabasal layers expressed markers of basal keratinocytes, including K5 and K14; β1, α6, and β4 integrins; and LM332, and were unevenly distributed. They were detected in areas where the epidermis was firmly attached to the BM but also in epidermal stretches above microblisters. A similar hyperplastic epidermis was previously observed in transgenic mice ectopically expressing β1 integrin in the stratum granulosum (Carroll et al., 1995). The β1 transgenic keratinocytes were hyperproliferative, which was thought to be triggered by an excessive cytokine release from infiltrating inflammatory cells. Because we did not observe a chronic wounding response with an obvious inflammatory infiltrate (likely because the blistering was mild) at P7, when suprabasal proliferation was already evident, the proliferation and hyperplasia of the ILK-K5 epidermis must be triggered by a different

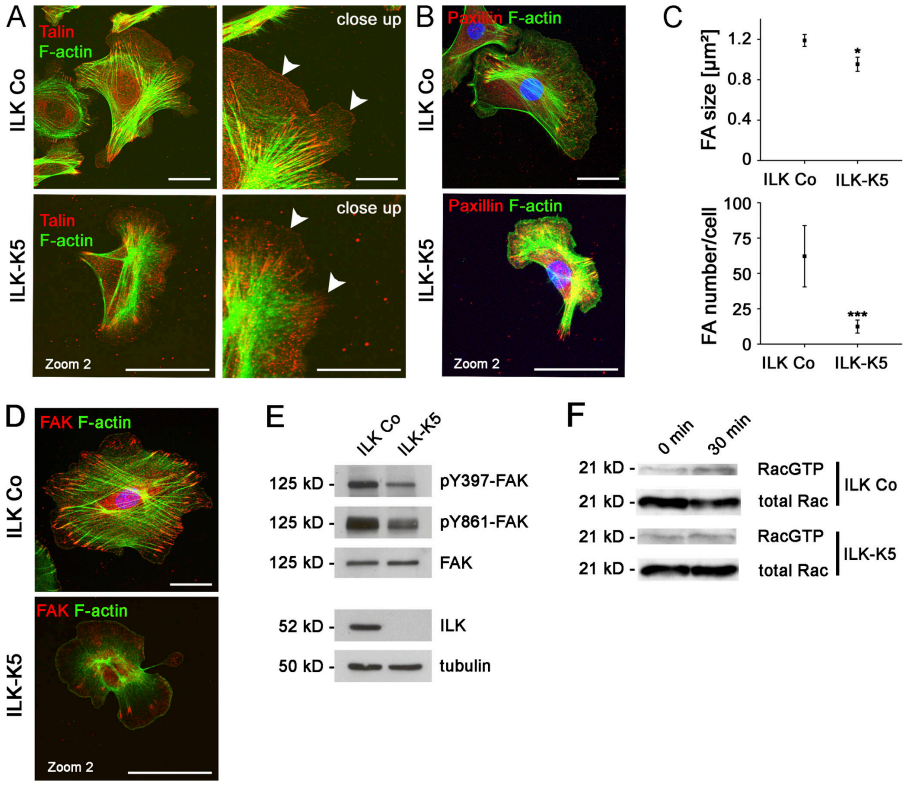

Figure 9. **Impaired formation of FAs but normal Rac1 activation in ILK-K5 keratinocytes.** (A, left) Immunostaining of primary control and ILK-K5 keratinocytes for talin and F-actin. Control and ILK-K5 keratinocytes contain talin in FAs. ILK-K5 cells are enlarged twofold compared with control cells. Bars, 10 µm. (right) A close up demonstrates talin in FCs at the leading edge of control cells (arrowheads). ILK-K5 keratinocytes have fewer talin-positive FCs at the leading edge (arrowheads). Bars, 2.5 µm. (B) Immunostaining of control and ILK-K5 keratinocytes for paxillin, F-actin, and DAPI. Bars, 10 µm. (C) Quantification of paxillin-containing FAs. ILK-K5 keratinocytes exhibit reduced size and amount of paxillin containing FAs compared with control keratinocytes. Error bars indicate 95% confidence interval of mean values. *, $P < 0.05$; ***, $P < 0.001$. (D) Immunostaining of primary control and ILK-K5 keratinocytes for FAK, F-actin, and DAPI. Note that mutant keratinocytes form fewer FAs that are poorly linked to thin and disorganized actin fibers. Bars, 10 µm. (E) Western blot analysis of protein lysates from primary keratinocytes showing reduced FAK phosphorylation levels in the absence of ILK. (F) Western blot analysis of a GTPase pull-down assay showing normal activation of Rac1 in primary ILK-K5 keratinocytes after 30 min of adhesion on a LM322-rich matrix.

mechanism. A possible explanation is that the proliferating basal keratinocytes detach because of an impaired adhesion strength, which leads to their ectopic location and marked thickening of the epidermis. It could also be that an accelerated proliferation rate contributes to the ectopic distribution of proliferating keratinocytes. Such a notion is supported by the elevated proliferation rate of primary keratinocytes in vitro. However, it is currently unclear why ILK-K5 keratinocytes would proliferate better than their normal control counterparts. Finally, delayed terminal differentiation of suprabasal keratinocytes may additionally contribute to the epidermal hyperplasia. In ILK-K5 epidermis, the K5- and K14-positive keratinocyte zone extended into several layers of the K10-positive stratum granulosum. Also the loricrin-positive cell compartment was increased. Interestingly, epidermal thickening and delay in keratinocyte differentiation was also observed in the β1 integrin–deficient epidermis (Brakebusch et al., 2000). In contrast to the ILK-K5 skin, however, the hyperthickened, β1 integrin–null epidermis contained fewer proliferating basal keratinocytes (Brakebusch et al., 2000; Raghavan et al., 2000), suggesting that β1 integrins accomplish keratinocyte differentiation through ILK and keratinocyte proliferation through an ILK-independent mechanism.

The diminished integrin-mediated attachment of keratinocytes to the BM resulted in blister formation, deterioration of the BM, and abnormal distribution of E-cadherin and β-catenin above blisters. In attached epidermis, E-cadherin and β-catenin were normally distributed, suggesting that ILK affects E-cadherin–based cell–cell adhesion structures rather indirectly. This is in contrast to previous reports showing that ILK regulates E-cadherin expression (Tan et al., 2001) and assembly of E-cadherin–based cell–cell adhesions (Vespa et al., 2005).

HF development and cycling

The most impressive phenotype of ILK-K5 mice is their progressive hair loss, which is completed at the age of 6–8 wk. Upon completion of morphogenesis, ILK-K5 skin revealed two types of abnormal HFs: long HFs with multilayered ORS and short, immature HFs that were stuck in the dermis. The existence of two types of HFs is most easily explained by the asynchronous development of HFs over a period of several days. The depletion of the ILK protein around birth is consequently hitting HFs later (long HFs; Figs. 2, 5, and 6, ▲) or earlier (short HFs; Figs. 2, 5, and 6, ■) in their development. In both types of HFs, although much more pronounced in long HFs, we observed an accumulation of proliferating cells in the hyperthickened ORS. The concomitant reduction of proliferating cells in the HM and the presence of CD34-postive stem cells in the hair bulge suggest that TA cells are generated but fail to migrate down to and replenish the HM, arresting HF development and maintenance. It is conceivable that hyperproliferation, like in the epidermis, may additionally contribute to the hyperthickening of the ORS.

We also observed abnormal localization of DPs during HF morphogenesis and detachment of the DP from ∼35% ILK-K5 HFs in P24 mice. Because the DP is releasing signals that are required for HF development and maintenance (Panteleyev et al., 1998), such abnormalities are likely to contribute to the hair loss. Interestingly, ILK-K5 HFs still connected to the DP could respond to the inductive signals and trigger sustained proliferation. In spite of the successful induction of anaphase, however, downward migration of the mutant HF epithelium was never observed.

What could be the underlying mechanism for the defective migration? Our analysis of primary keratinocytes revealed that loss of ILK alters the formation of mature FAs and prevents persistent, directional migration. Single-cell imaging demonstrated that ILK-K5 keratinocytes are perfectly able to form membrane protrusions but are unable to stabilize them over a prolonged period of time. As a consequence, lamellipodia are short-lived and frequently collapse. Interestingly, ILK-K5 keratinocytes swiftly respond with the formation of new lamellipodia, often simultaneously at multiple sites of the cell. In vivo such a high turnover rate of lamellipodia would force migrating ILK-K5 ORS cells to continuously change the direction of movement, which, along with the reduced migration velocity, could explain their accumulation in the ORS and their handicap to arrive in the HM.

Molecularly, we found several defects that could account for the impaired directional persistence and migration speed. First, ILK-K5 keratinocytes showed weakened integrin adhesion, which could compromise the fixation of lamellipodia. Second, the defective formation of integrin adhesion sites could lessen integrin-signaling pathways crucial for cell migration, such as the activation of FAK. Third, diminished integrin signaling could, in turn, lead to an impaired spatiotemporal activation of small Rho-like GTPases. The stabilization of lamellipodia and directional migration of keratinocytes critically depends on the optimal activation of the small GTPase Rac1 (Nobes and Hall, 1999; Ridley et al., 2003). In vitro studies with human keratinocytes revealed that high Rac1 activity can lead to inefficient migration with low lamellipodia persistence (Borm et al., 2005). Likewise, reduced Rac1 activity in α3β1 integrin–deficient keratinocytes can also result in directional migration defects and short-lived leading-edge lamellipodia (Choma et al., 2004). The ILK-K5 keratinocytes show a normal Rac1 activation after seeding on a LM322-enriched ECM, indicating that either ILK is not required for modulating Rac1 activity in keratinocytes or we were unable to detect small but critical differences in Rac1 activation between control and ILK-K5 keratinocytes. Thus, we anticipate that loss of ILK is sufficient to compromise the dynamics of lamellipodia and FAs and, consequently, results in altered cell migration.

An abnormal proliferation rate of HM cells could also potentially contribute to hair loss in ILK-K5 mice. Loss of β1 integrins impairs ORS cell migration and proliferation of HM cells (Brakebusch et al., 2000; Raghavan et al., 2000). In sharp contrast, we found robust proliferation in the HM of short ILK-K5 HFs. In fully developed ILK-K5 HFs, the number of proliferating HM cells diminished with the accumulation of proliferating cells in the ORS. These findings, along with the increased proliferation rate of primary ILK-K5 keratinocytes in vitro, suggest that HM cell proliferation can be sustained in the absence of ILK.

ILK does not regulate GSK-3β activity in HFs

The inactivation of GSK-3β and the subsequent stability and nuclear translocation of β-catenin and formation of a Lef1–Tcf–β-catenin complex plays a fundamental role for the differentiation of the HM cells into the precortical HM and HS (DasGupta and Fuchs, 1999; Huelsken et al., 2001). The inactivation of GSK-3β and stabilization of β-catenin is achieved by Wnt signals (Logan and Nusse, 2004) or by ILK-dependent phosphorylation of GSK-3β (Delcommenne et al., 1998) and/or inhibition of the β-catenin destruction complex (Oloumi et al., 2006). Despite the high expression of ILK throughout the entire HM, we found no evidence for reduced GSK-3β phosphorylation in ILK-K5 keratinocytes, decreased β-catenin levels, diminished Lef1–Tcf–β-catenin activity (both in prematurely arrested as well as fully developed HFs), or impaired differentiation of HM keratinocytes into trichocytes. These findings indicate that, contrary to what has been reported for intestinal and mammary epithelial cells (Novak et al., 1998) and for HEK293 and L2 cells, ILK is not required to stabilize β-catenin in the HF epithelium to induce expression of HS keratins. These findings, along with recent observations in mice with other organ-specific ILK deletions (Grashoff et al., 2003; Niewmierzycka et al., 2005), suggest that the ILK activity, at least toward GSK-3β and PKB/Akt, may not be required under physiological conditions in vivo.

Materials and methods

Mouse strains

To obtain mice with a keratinocyte-restricted deletion of the ILK gene, transgenic mice expressing *Cre* under the control of the keratin-5 promoter (Brakebusch et al., 2000) were crossed with floxed ILK mice (Grashoff et al., 2003; Sakai et al., 2003). Offspring were genotyped as described previously (Grashoff et al., 2003). BatGal transgenic mice carry Lef1/Tcf binding sites in front of a minimal promoter and the *lacZ* gene (Maretto et al., 2003) and were intercrossed with the ILK mutant mice.

Keratinocyte, epidermal lysate, and GTPase pull-down assay

Primary keratinocytes were cultured in keratinocyte growth medium containing 8% FCS and low Ca^{2+} (45 μM) on cell culture dishes coated with a mixture of Col I (Cohesion) and FN (Invitrogen) to subconfluence as described previously (Romero et al., 1999). Protein lysates from keratinocytes or epidermis were separated by SDS gel electrophoresis, blotted, and incubated with the indicated antibodies.

For GTPase pull-down assays, keratinocytes were cultivated to 70% confluence. Cells were then serum starved overnight and detached by Trypsin/EDTA treatment (Invitrogen). Detached cells were resuspended in serum-free keratinocyte growth medium and kept for 30 min in suspension. For adhesion-induced GTPase activation, cells were plated on a LM332-rich matrix produced by Rac-11P/SD squamous cell carcinoma cells for 30 min (Sonnenberg et al., 1993). Cells were washed twice with PBS and then lysed in lysis buffer (50 mM Tris-HCl, pH 7.4, 100 mM NaCl, 1% Nonidet P-40, 10% glycerol, 2 mM $MgCl_2$, 1 mM NaF, and 1 mM Na_3VO_4; all from Sigma-Aldrich) supplemented with protease inhibitor cocktail tablets (Complete Mini, EDTA-free; Roche) and containing biotinylated PAK-CRIB peptide (a gift from J. Collard, Netherlands Cancer Institute, Amsterdam, Netherlands). Lysates were centrifuged at 20,000 *g* for 10 min at 4°C, and the supernatant was subsequently incubated for 45 min at 4°C. Next, lysates were incubated with streptavidin-conjugated agarose beads (GE Healthcare) for 30 min at 4°C. Beads were washed three times with lysis buffer, resuspended in 2× SDS sample buffer, and boiled for 5 min at 95°C. The supernatant was subjected to SDS gel electrophoresis, Western blotting, and immunodetection by the indicated antibodies. The following antibodies were used for Western blot analysis: mouse mAb against ILK (clone 3; BD Biosciences); rat mAb against α-tubulin (Kilmartin et al., 1982); rabbit pAb against PKB/Akt and phospho-PKB/Akt (Ser473; Cell Signaling Technology); mouse mAb against GSK-3β (BD Biosciences); rabbit pAb against phospho–GSK-3β (Ser9; Biosource International); mouse mAb against cyclin D1/2 (Upstate Biotechnology); rabbit pAb against cyclin A (Santa Cruz Biotechnology, Inc.); rabbit pAb against p42/44 MAPK (Cell Signaling Technology); mouse mAb against phospho-p42/44 MAPK Thr202/204 (New England Biolabs, Inc.); rat mAb against E-cadherin (Zymed Laboratories); rabbit pAb against β-catenin (Sigma-Aldrich); rabbit pAbs against FAK (Upstate Biotechnology) and pFAK (Tyr397and Tyr861; Biosource International); mouse mAb against Rac1 (BD Biosciences); and goat anti–rat HRP, goat anti–mouse HRP, and goat anti–rabbit HRP (Bio-Rad Laboratories).

Histology and immunohistochemistry

Skin samples were fixed in 4% PFA in PBS, pH 7.2, overnight, dehydrated in a graded alcohol series, and embedded in paraffin (Paraplast X-tra; Sigma-Aldrich) or frozen unfixed in OCT (Thermo Shandon). Immunohistochemistry of skin sections was performed as described previously (Brakebusch et al., 2000). For cellular immunostainings, keratinocytes were seeded on chamber slides (Nunc) coated with 5 μg/ml of purified LM332 or 30 μg/ml Col I and 10 μg/ml FN and allowed to spread for 40 h. Cells were washed in PBS, fixed in 4% PFA, and incubated with the indicated antibodies. To determine BrdU incorporation, mice were injected with BrdU (100 μg/g body weight) 2 h before killing. Assessment of proliferation of cultured keratinocytes was performed with the Cell Proliferation ELISA according to the manufacturer's protocol (Roche). The following antibodies were used for immunohistology: rabbit pAb against ILK (Cell Signaling Technology); FITC-conjugated mAb against integrin α6 (BD Biosciences); rat mAb against β1 integrin (Chemicon); rat mAb against β4 integrin (BD Biosciences); rabbit pAb against laminin-5 (Brakebusch et al., 2000); rabbit pAbs against keratins 6, 10, and 14 and loricrin (Covance); rat mAb against E-cadherin; rabbit pAb against β-catenin; rabbit pAb β-catenin (Huelsken et al., 2000); rat mAb against nidogen (Chemicon); rabbit pAb against desmoplakin (Research Diagnostics); rabbit pAb against plakoglobin (Santa Cruz Biotechnology, Inc.); rabbit pAb against Lef1 (obtained from R. Grosschedl, Max Planck Institute of Immunobiology, Freiburg, Germany); rat Ki67 (Dianova); guinea pig pAbs against HF keratins (K6hf, K6irs1, K6irs2, K6irs3, K6irs4, hHa4, hHa5, hHb2, hHb5, CK5, and CK14; made by L. Langbein, German Cancer Research Center, Heidelberg, Germany); rat mAb against CD34 (clone RAM34; eBioscience); FITC-conjugated mouse mAb and POD-conjugated mAb against BrdU (Roche); rabbit pAb against cleaved caspase-3 (Asp175; Cell Signaling Technology); mouse mAb against paxillin (BD Biosciences); rabbit pAbs against FAK (Upstate Biotechnology) and phospho-FAK (Tyr397 and Tyr861; Biosource International); mouse mAb against Talin (Sigma-Aldrich); phalloidin Alexa488 (Invitrogen); goat anti–mouse Cy3, goat anti–rat Cy3, goat anti–rabbit FITC, and donkey anti–rabbit Cy3 (Jackson ImmunoResearch Laboratories); goat anti–rabbit Alexa488 (Sigma-Aldrich); and goat anti–rat Alexa488 (Invitrogen). Images were collected at room temperature by confocal microscopy (DMIRE2; Leica) using the Leica Confocal Software (version 2.5 Build 1227) with 63× NA 1.4 or 100× NA 1.4 oil objectives or by bright field microscopy (Axioskop; Carl Zeiss MicroImaging, Inc.) with 10× NA 0.3, 20× NA 0.5, or 40× NA 0.75 objectives, a camera (DC500; Leica), and IM50 software.

FACS analysis

Flow cytometry was performed as described by Brakebusch et al. (2000). Antibodies used for FACS analysis are as follows: FITC-conjugated hamster mAb against integrin β1; rat mAb against integrin β1 9EG7; FITC-conjugated rat mAb against integrin α6; biotinylated rat mAb against integrin αV; rat mAb against integrin β4; FITC-conjugated hamster mAb against integrin α2; biotinylated rat mAb against integrin α5 (all obtained from BD Biosciences); mouse mAb against integrin α3 (BD Biosciences); Streptavidin-Cy5 (BD Biosciences); mouse mAb anti–rat FITC (BD Biosciences); and goat anti–mouse FITC (Jackson ImmunoResearch Laboratories).

Adhesion and transwell assays

Adhesion of epidermal keratinocytes to ECM proteins (poly-L-lysine [Sigma-Aldrich], Col I, Col IV [a gift from R. Timpl, Max Planck Institute of Biochemistry, Martinsried, Germany], FN, and LM332) was measured as described previously (Fässler et al., 1995). Transwell migration and matrigel invasion assays of primary keratinocytes were performed as described by Thomas et al. (2001).

Cell-wounding assay

Monolayers were treated with 4 μg/ml Mitomycin C (Sigma-Aldrich) for 4 h before scratching with a 200-μl plastic micropipette to obtain wound

widths of 500–600 μm. Live-cell recordings were performed immediately after wounding for 12 h at 37°C and 5% CO_2 using a microscope (Axiovert; Carl Zeiss MicroImaging, Inc.) equipped with 10× NA 0.3, 20× NA 0.4, 40× NA 0.6, and 100× NA 1.3 objectives, motorized scanning table (Märzhäuser) and a stage incubator (EMBL Precision Engineering). Images were captured every 10 min with a cooled charge-coupled device camera (MicroMAX; Roper Scientific) using the MetaMorph software (Universal Imaging Corp.) for microscope control and data acquisition. Wound closure was quantified by measuring the distance between both leading edges moving toward the wound in 20 randomly chosen regions. At least four independent scratch-wound experiments were used for calculations. Migration velocity was determined by calculating the slope of a linear regression line. Single-cell tracking of cells within the leading edge was performed using MetaMorph software, choosing 15 cells each in at least three independent experiments.

Cell spreading

Cells were seeded on Col I/FN-coated dishes (MatTek Corporation) and allowed to spread for the indicated time. Four images were taken by the live-cell recording unit for each time point, and cell area was assessed using MetaMorph software.

Kymograph analysis

Lamellipodia dynamics and lamella stability was analyzed using kymography (Hinz et al., 1999). We monitored at least 10 migrating cells over a period of 20 min with a frame rate of 4 s using the live-cell imaging unit (100× NA 1.3 objective). Subsequently, eight areas of interest across the cell lamella with a 1-pixel width were defined. The 1-pixel-wide images were pasted side-by-side to generate a composite image of membrane dynamic at a single point along the cell lamella. As described by Hinz et al. (1999), slopes of these lines were used to calculate the velocities, and projections of these lines along the x axis (time) were used to calculate the persistence of protrusions.

Transmission EM

Transmission EM was performed as described previously (Grose et al., 2002).

Statistical analysis

Statistical evaluation was performed with SPSS software (SPSS, Inc). Statistical significance between data groups was determined by Whitney U test and subdivided into three groups (*, $P < 0.05$; **, $P < 0.01$; ***, $P < 0.001$).

Online supplemental material

Fig. S1 shows the ILK expression on newborn and 2-d-old skin sections and the integrin-expression pattern on freshly isolated control and ILK-K5 keratinocytes. Fig. S2 shows the numbers of proliferating cells in basal and suprabasal layers of control and ILK-K5 epidermis, in vitro proliferation of primary control and ILK-K5 keratinocytes, and the phosphorylation levels of GSK-3β and PKB/Akt. Fig. S3 shows immunostaining for Mac1 and Gr1 on skin sections of 7-d- and 2-wk-old mice and transmission EM of desmosomal contacts in the epidermis. Fig. S4 shows the integrin-expression pattern and immunostaining for integrins on cultured primary control and ILK-K5 keratinocytes and spreading kinetics of freshly isolated keratinocyte. Video 1 shows time-lapse video microscopy of control keratinocytes. Video 2 shows time-lapse video microscopy of ILK-K5 keratinocytes. Online supplemental material is available at http://www.jcb.org/cgi/content/full/jcb.200608125/DC1.

We thank Michal Grzejszczyk, Simone Bach, and Keiko Sakai for expert technical assistance; Dr. Stefano Piccolo (University of Padua, Padua, Italy) for the BatGal mice; Dr. Joerg Huelsken (Swiss Institute for Experimental Cancer Research, Epalinges, Switzerland) for the β-catenin antibody; Dr. John Collard (The Netherlands Cancer Institute, Amsterdam, Netherlands) for the PAK-CRIB peptide; and Drs. Kyle Legate, Ingo Thievessen, and Ralf Paus for discussions and critically reading the manuscript.

This work was supported by Bundesministerium für Bildung und Forschung, Deutsche Forschungsgemeinschaft, and the Max Planck Society.

Submitted: 21 August 2006
Accepted: 5 April 2007

References

Auber, L. 1952. The anatomy of follicles producing wool-fibres, with special reference to keratinization. *Trans. Royal Soc. Edinburgh.* 62:191–254.

Blanpain, C., and E. Fuchs. 2006. Epidermal stem cells of the skin. *Annu. Rev. Cell Dev. Biol.* 22:339–373.

Borm, B., R.P. Requardt, V. Herzog, and G. Kirfel. 2005. Membrane ruffles in cell migration: indicators of inefficient lamellipodia adhesion and compartments of actin filament reorganization. *Exp. Cell Res.* 302:83–95.

Brakebusch, C., and R. Fässler. 2003. The integrin-actin connection, an eternal love affair. *EMBO J.* 22:2324–2333.

Brakebusch, C., R. Grose, F. Quondamatteo, A. Ramirez, J.L. Jorcano, A. Pirro, M. Svensson, R. Herken, T. Sasaki, R. Timpl, et al. 2000. Skin and hair follicle integrity is crucially dependent on β1 integrin expression on keratinocytes. *EMBO J.* 19:3990–4003.

Carroll, J.M., M.R. Romero, and F.M. Watt. 1995. Suprabasal integrin expression in the epidermis of transgenic mice results in developmental defects and a phenotype resembling psoriasis. *Cell.* 83:957–968.

Choma, D.P., K. Pumiglia, and C.M. DiPersio. 2004. Integrin α3β1 directs the stabilization of a polarized lamellipodium in epithelial cells through activation of Rac1. *J. Cell Sci.* 117:3947–3959.

Commo, S., and B.A. Bernard. 1997. The distribution of α2β1, α3β1 and α6β4 integrins identifies distinct subpopulations of basal keratinocytes in the outer root sheath of the human anagen hair follicle. *Cell. Mol. Life Sci.* 53:466–471.

DasGupta, R., and E. Fuchs. 1999. Multiple roles for activated LEF/TCF transcription complexes during hair follicle development and differentiation. *Development.* 126:4557–4568.

Delcommenne, M., C. Tan, V. Gray, L. Rue, J. Woodgett, and S. Dedhar. 1998. Phosphoinositide-3-OH kinase-dependent regulation of glycogen synthase kinase 3 and protein kinase B/AKT by the integrin-linked kinase. *Proc. Natl. Acad. Sci. USA.* 95:11211–11216.

Fässler, R., M. Pfaff, J. Murphy, A.A. Noegel, S. Johansson, R. Timpl, and R. Albrecht. 1995. Lack of β1 integrin gene in embryonic stem cells affects morphology, adhesion, and migration but not integration into the inner cell mass of blastocysts. *J. Cell Biol.* 128:979–988.

Fuchs, E., and S. Raghavan. 2002. Getting under the skin of epidermal morphogenesis. *Nat. Rev. Genet.* 3:199–209.

Fuchs, E., B.J. Merrill, C. Jamora, and R. DasGupta. 2001. At the roots of a never-ending cycle. *Dev. Cell.* 1:13–25.

Grashoff, C., A. Aszodi, T. Sakai, E.B. Hunziker, and R. Fässler. 2003. Integrin-linked kinase regulates chondrocyte shape and proliferation. *EMBO Rep.* 4:432–438.

Grashoff, C., I. Thievessen, K. Lorenz, S. Ussar, and R. Fässler. 2004. Integrin-linked kinase: integrin's mysterious partner. *Curr. Opin. Cell Biol.* 16:565–571.

Grose, R., C. Hutter, W. Bloch, I. Thorey, F.M. Watt, R. Fässler, C. Brakebusch, and S. Werner. 2002. A crucial role of β1 integrins for keratinocyte migration in vitro and during cutaneous wound repair. *Development.* 129:2303–2315.

Hannigan, G.E., C. Leung-Hagesteijn, L. Fitz-Gibbon, M.G. Coppolino, G. Radeva, J. Filmus, J.C. Bell, and S. Dedhar. 1996. Regulation of cell adhesion and anchorage-dependent growth by a new β1 integrin-linked protein kinase. *Nature.* 379:91–96.

Hill, M.M., J. Feng, and B.A. Hemmings. 2002. Identification of a plasma membrane Raft-associated PKB Ser473 kinase activity that is distinct from ILK and PDK1. *Curr. Biol.* 12:1251–1255.

Hinz, B., W. Alt, C. Johnen, V. Herzog, and H.W. Kaiser. 1999. Quantifying lamella dynamics of cultured cells by SACED, a new computer-assisted motion analysis. *Exp. Cell Res.* 251:234–243.

Huelsken, J., R. Vogel, V. Brinkmann, B. Erdmann, C. Birchmeier, and W. Birchmeier. 2000. Requirement for β-catenin in anterior-posterior axis formation in mice. *J. Cell Biol.* 148:567–578.

Huelsken, J., R. Vogel, B. Erdmann, G. Cotsarelis, and W. Birchmeier. 2001. β-Catenin controls hair follicle morphogenesis and stem cell differentiation in the skin. *Cell.* 105:533–545.

Kilmartin, J.V., B. Wright, and C. Milstein. 1982. Rat monoclonal antitubulin antibodies derived by using a new nonsecreting rat cell line. *J. Cell Biol.* 93:576–582.

Legate, K.R., E. Montanez, O. Kudlacek, and R. Fässler. 2006. ILK, PINCH and parvin: the tIPP of integrin signalling. *Nat. Rev. Mol. Cell Biol.* 7:20–31.

Logan, C.Y., and R. Nusse. 2004. The Wnt signaling pathway in development and disease. *Annu. Rev. Cell Dev. Biol.* 20:781–810.

Lynch, D.K., C.A. Ellis, P.A. Edwards, and I.D. Hiles. 1999. Integrin-linked kinase regulates phosphorylation of serine 473 of protein kinase B by an indirect mechanism. *Oncogene.* 18:8024–8032.

Mackinnon, A.C., H. Qadota, K.R. Norman, D.G. Moerman, and B.D. Williams. 2002. *C. elegans* PAT-4/ILK functions as an adaptor protein within integrin adhesion complexes. *Curr. Biol.* 12:787–797.

Maretto, S., M. Cordenonsi, S. Dupont, P. Braghetta, V. Broccoli, A.B. Hassan, D. Volpin, G.M. Bressan, and S. Piccolo. 2003. Mapping Wnt/β-catenin signaling during mouse development and in colorectal tumors. *Proc. Natl. Acad. Sci. USA.* 100:3299–3304.

Niewmierzycka, A., J. Mills, R. St-Arnaud, S. Dedhar, and L.F. Reichardt. 2005. Integrin-linked kinase deletion from mouse cortex results in cortical lamination defects resembling cobblestone lissencephaly. *J. Neurosci.* 25:7022–7031.

Nobes, C.D., and A. Hall. 1999. Rho GTPases control polarity, protrusion, and adhesion during cell movement. *J. Cell Biol.* 144:1235–1244.

Novak, A., S.C. Hsu, C. Leung-Hagesteijn, G. Radeva, J. Papkoff, R. Montesano, C. Roskelley, R. Grosschedl, and S. Dedhar. 1998. Cell adhesion and the integrin-linked kinase regulate the LEF-1 and β-catenin signaling pathways. *Proc. Natl. Acad. Sci. USA*. 95:4374–4379.

Oloumi, A., S. Syam, and S. Dedhar. 2006. Modulation of Wnt3a-mediated nuclear β-catenin accumulation and activation by integrin-linked kinase in mammalian cells. *Oncogene.* 25:7747–7757.

Panteleyev, A.A., C. van der Veen, T. Rosenbach, S. Muller-Rover, V.E. Sokolov, and R. Paus. 1998. Towards defining the pathogenesis of the hairless phenotype. *J. Invest. Dermatol.* 110:902–907.

Paus, R., and G. Cotsarelis. 1999. The biology of hair follicles. *N. Engl. J. Med.* 341:491–497.

Paus, R., S. Muller-Rover, C. Van Der Veen, M. Maurer, S. Eichmuller, G. Ling, U. Hofmann, K. Foitzik, L. Mecklenburg, and B. Handjiski. 1999. A comprehensive guide for the recognition and classification of distinct stages of hair follicle morphogenesis. *J. Invest. Dermatol.* 113:523–532.

Persad, S., S. Attwell, V. Gray, M. Delcommenne, A. Troussard, J. Sanghera, and S. Dedhar. 2000. Inhibition of integrin-linked kinase (ILK) suppresses activation of protein kinase B/Akt and induces cell cycle arrest and apoptosis of PTEN-mutant prostate cancer cells. *Proc. Natl. Acad. Sci. USA.* 97:3207–3212.

Raghavan, S., C. Bauer, G. Mundschau, Q. Li, and E. Fuchs. 2000. Conditional ablation of β1 integrin in skin: severe defects in epidermal proliferation, basement membrane formation, and hair follicle invagination. *J. Cell Biol.* 150:1149–1160.

Ridley, A.J., M.A. Schwartz, K. Burridge, R.A. Firtel, M.H. Ginsberg, G. Borisy, J.T. Parsons, and A.R. Horwitz. 2003. Cell migration: integrating signals from front to back. *Science.* 302:1704–1709.

Romero, M.R., J.M. Caroll, and F.M. Watt. 1999. Analysis of cultured keratinocytes from a transgenic mouse model of psoriasis: effects of suprabasal integrin expression on keratinocyte adhesion, proliferation and terminal differentiation. *Exp. Dermatol.* 8:53–67.

Sakai, T., S. Li, D. Docheva, C. Grashoff, K. Sakai, G. Kostka, A. Braun, A. Pfeifer, P.D. Yurchenco, and R. Fässler. 2003. Integrin-linked kinase (ILK) is required for polarizing the epiblast, cell adhesion, and controlling actin accumulation. *Genes Dev.* 17:926–940.

Sonnenberg, A., A.A. de Melker, A.M. Martinez de Velasco, H. Janssen, J. Calafat, and C.M. Niessen. 1993. Formation of hemidesmosomes in cells of a transformed murine mammary tumor cell line and mechanisms involved in adherence of these cells to laminin and kalinin. *J. Cell Sci.* 106:1083–1102.

Tan, C., P. Costello, J. Sanghera, D. Dominguez, J. Baulida, A.G. de Herreros, and S. Dedhar. 2001. Inhibition of integrin linked kinase (ILK) suppresses β-catenin-Lef/Tcf-dependent transcription and expression of the E-cadherin repressor, snail, in APC−/− human colon carcinoma cells. *Oncogene.* 20:133–140.

Thomas, G.J., M.P. Lewis, S.A. Whawell, A. Russell, D. Sheppard, I.R. Hart, M. Speight, and J.F. Marshall. 2001. Expression of the αvβ6 integrin promotes migration and invasion in squamous carcinoma cells. *J. Invest. Dermatol.* 117:67–73.

Troussard, A.A., P.C. McDonald, E.D. Wederell, N.M. Mawji, N.R. Filipenko, K.A. Gelmon, J.E. Kucab, S.E. Dunn, J.T. Emerman, M.B. Bally, and S. Dedhar. 2006. Preferential dependence of breast cancer cells versus normal cells on integrin-linked kinase for protein kinase B/Akt activation and cell survival. *Cancer Res.* 66:393–403.

Vespa, A., S.J. D'Souza, and L. Dagnino. 2005. A novel role for integrin-linked kinase for epithelial sheet morphogenesis. *Mol. Biol. Cell.* 16:4084–4095.

Watt, F.M. 2002. Role of integrins in regulating epidermal adhesion, growth and differentiation. *EMBO J.* 21:3919–3926.

Zervas, C.G., S.L. Gregory, and N.H. Brown. 2001. *Drosophila* integrin-linked kinase is required at sites of integrin adhesion to link the cytoskeleton to the plasma membrane. *J. Cell Biol.* 152:1007–1018.

Zhou, P., C. Byrne, J. Jacobs, and E. Fuchs. 1995. Lymphoid enhancer factor 1 directs hair follicle patterning and epithelial cell fate. *Genes Dev.* 9:700–713.